X-611-66-226

NASA TM X-55500

SOLAR MODULATION OF GALACTIC COSMIC RAYS

GPO PRICE $ ______

CFSTI PRICE(S) $ ______

Hard copy (HC) 2.00

Microfiche (MF) .50

ff 653 July 65

MAY 1966

FACILITY FORM 602

N66 29968 (ACCESSION NUMBER)	(THRU)
38 (PAGES)	1 (CODE)
TM-X ~~54408~~ 55500 (NASA CR OR TMX OR AD NUMBER)	29 (CATEGORY)

NASA

GODDARD SPACE FLIGHT CENTER

GREENBELT, MD.

SOLAR MODULATION OF GALACTIC COSMIC RAYS

by

V. K. Balasubrahmanyan, E. Boldt,

and

R. A. R. Palmeira

Goddard Space Flight Center

Greenbelt, Maryland

SOLAR MODULATION OF GALACTIC COSMIC RAYS

by

V. K. Balasubrahmanyan,[1] E. Boldt,

and

R. A. R. Palmeira[2]

Goddard Space Flight Center,

Greenbelt, Maryland

ABSTRACT

The modulation of galactic protons and He nuclei during the last solar cycle is analyzed according to Parker's theory. The mechanism of modulation remains essentially the same during several years of low solar activity (1961-1965). The modulation near solar maximum (1959) implies that the scale sizes of the magnetic inhomogeneities in the solar wind are reduced below the values at solar minimum. An adequate description at solar maximum would require further refinements of the theory. The proton to He nucleus ratio outside the solar system is shown to be consistent with a value ≈ 6, in a kinetic-energy/nucleon representation for the interval 50 to 1000 Mev/nucleon.

---

[1]On leave from Tata Institute of Fundamental Research, Bombay, India.

[2]NAS-NASA Post-Doctoral Resident Research Associate, on leave from Centro Brasileiro de Pesquisas Fisicas, Rio de Janeiro, Brazil. Present address: Southwest Center for Advanced Studies, Dallas, Texas.

INTRODUCTION

Since the discovery by Forbush [1954] of the inverse correlation of cosmic ray intensity with solar activity, many experimental and theoretical studies of the long term solar modulation effects on galactic cosmic radiation have been attempted. The present status of the subject has been presented in several recent reviews, [Webber, 1964; Quenby, 1964] as well as in some recent papers [Fichtel et al., 1965; Freier and Waddington, 1965; Nagashima et al., 1966]. In this paper we analyze the available energy spectrum data obtained during the last solar cycle to see how far they conform to the predictions of the theory of the cosmic ray modulation caused by the solar wind [Parker 1963]. It is considered pertinent to do this as recent satellite measurements [Bonnetti et al., 1963; Ness et al., 1964, 1966] have confirmed the existence of the solar wind, the solar origin of the interplanetary magnetic field and the convection of magnetic inhomogeneities of the right size to modulate galactic cosmic rays.

PARKER'S THEORY OF THE 11-YEAR SOLAR MODULATION

Parker [1963] has developed a theory of the 11-year cosmic-ray variation in which the cosmic ray density at the earth's orbit is determined by the steady state equilibrium between the inward diffusion of galactic cosmic rays and their outward convection by the solar wind. Assuming spherical symmetry Parker arrives at the following equation relating the cosmic ray density at the orbit of the earth $\mu_e(\beta)$ to the cosmic ray density outside the solar influence $\mu_\infty(\beta)$:

$$\mu_e(\beta) = \mu_\infty(\beta) \exp\left[-\int_{r_e}^{\infty} \frac{V(r)}{D(r, \beta)} dr\right] \tag{1}$$

where $V(r)$ is the solar wind velocity and $D(r, \beta)$ is the diffusion coefficient, and r_e the distance of the earth from the sun. In general $D(r, \beta)$ is a function of the radial distance r and the particle velocity βc given by

$$D(r, \beta) = \beta c \lambda(r, \beta) \tag{2}$$

where $\lambda(r, \beta)$ is the mean free path for the diffusion process. For an arbitrary distribution of the scale size characterizing the inhomogeneities in the magnetic field

$$\frac{1}{\lambda(r, \beta)} = \int_0^{\infty} \sigma(\ell, \beta)\, \rho(\ell, r)\, d\ell \tag{3}$$

where $\sigma(\ell, \beta)$ is the effective cross-section for the scattering of a particle with velocity βc by an inhomogeneity in the magnetic field with a scale size ℓ, and $\rho(\ell, r)\, d\ell$ is the spatial density of scattering centers with scale sizes between ℓ and $\ell + d\ell$, at a distance r.

We assume that $\rho(\ell, r)$ is a separable function of ℓ and r;

$$\rho(\ell, r) = n(r)\, N(\ell) \tag{4}$$

where

$$\int_0^{\infty} N(\ell)\, d\ell = 1$$

We then have

$$M(\beta) \equiv \frac{\mu_e(\beta)}{\mu_\infty(\beta)} = \exp\left\{-\frac{1}{\beta}\left[\int_0^\infty \sigma(\ell, \beta) N(\ell)\, d\ell\right] \cdot \left[\int_{r_e}^\infty \frac{3V(r)\, n(r)}{c}\, dr\right]\right\} \tag{5}$$

In order to compare this modulation function with the observations, we need to specify a scattering cross-section $\sigma(\ell, \beta)$ and a distribution $N(\ell)$ of the scale size of the inhomogeneities.

Parker [1963] adopted

$$\sigma(\ell, \beta) = \begin{cases} \ell^2 & \text{for } R \leq \ell \quad (6a) \\ (\ell^4/R^2) & \text{for } R > \ell \quad (6b) \end{cases}$$

$$N(\ell) = \delta(\ell - \ell_0) \tag{7}$$

where R is the radius of curvature of a particle in a magnetic field B assumed independent of r:

$$R = \frac{pc}{ZeB} = \frac{A}{Z} m_0 c^2 \frac{\beta}{(1-\beta^2)^{1/2}} \cdot \frac{1}{eB} \tag{8}$$

where A and Z are the particle mass and charge numbers respectively and m_0 is the proton rest mass.

With this choice of $\sigma(\ell, \beta)$ and $N(\ell)$ we can write

$$M(\beta) = \exp\left(-\frac{K}{\beta}\right) \text{ for } \beta \leq \beta_0 \tag{9}$$

$$M(\beta) = \exp\left[-\frac{K}{\beta^3}\,(1-\beta^2)\left(\frac{\ell_0}{R_0}\right)^2\left(\frac{Z}{A}\right)^2\right] \text{ for } \beta > \beta_0 \tag{10}$$

where

$$K = \ell_0^2 \int_{r_e}^{\infty} \frac{3\,V(r)\,n(r)}{c}\,dr \tag{11}$$

$$R_0 = \frac{m_0\,c^2}{eB} \tag{12}$$

and

$$\beta_0 = \frac{(\ell_0 Z/R_0 A)}{\left[1 + (\ell_0 Z/R_0 A)^2\right]^{1/2}} \tag{13}$$

In the appendix we write the modulation function $M(\beta)$ for the more general case where the magnetic field B is a function of the radial distance r and $N(\ell)$ is a general distribution function. The formula so obtained is presented for the limits $\beta \rightarrow 0$ and $\beta \rightarrow 1$, where the influence of the radial dependence of B and of the choice of the distribution $N(\ell)$ is made more explicit.

EXPERIMENTAL DATA DURING THE PERIOD OF LOW SOLAR ACTIVITY

Figure 1 shows the Mt. Washington neutron monitor counting rate (courtesy of Dr. J. Lockwood, University of New Hampshire) and the sunspot number during the last solar cycle. The arrows indicate the times of balloon flights from which the balloon data used in this paper were obtained. The hatched region shows the time of the coverage provided by the IMP-I, II and III, and OGO-I satellites.

Figure 2 shows the proton and helium nucleus energy spectra in a kinetic energy per nucleon representation. The helium nucleus flux was multiplied by 5. The curve labeled 1963 has the analytical form

$$N(E)\,dE = \frac{10^8 \times E^{1.5}}{(E + 500)^4}\,dE \tag{14}$$

when E is in Mev. Equation 14 was constructed to fit the experimental data shown, and to have the asymptotic form $N(E) \propto E^{-2.5}$ at high energies [Balasubrahmanyan et al., 1965 b]. From this curve labeled 1963 we constructed the curve lableled 1965 by assuming that $\Delta K_{1965} \equiv K_{1965} - K_{1963} = -0.2$. In a like manner we constructed the curve labeled 1961, for $\Delta K_{1961} = +0.4$.

These data suggest that in the energy range of the observations and at a time near minimum solar activity, the solar modulation is predominantly velocity dependent. Studying the time variation of the low energy He nucleus spectrum Fan et al., [1965a] , and Gloeckler [1965], arrived at a similar conclusion, for energies up to 500 Mev/nucleon. The velocity β_0, at which the modulation function changes from pure velocity dependence to a mixture of velocity and rigidity dependence, is a function (equation 13) of (ℓ_0 / R_0). The experimental data indicate that up to approximately 1 Bev/nucleon the modulation is only velocity dependent. From this we conclude that from 1961 through 1965 the scale size of the inhomogeneities was such that

$(\ell_0/R_0) \geq 2$. For $\beta = 5\gamma \equiv 5 \times 10^{-5}$ gauss, this conclusion leads to $\ell_0 \geq 10^{-2}$ AU.

In addition to the low energy detectors, the satellites IMP-I, IMP-II, IMP-III and OGO-I carried GM counter telescopes of identical construction. When the telescopes were calibrated with the sea-level cosmic-ray muon flux the counting rates agreed within 1%. Details of these GM counter telescopes are given elesewhere [Balasubrahmanyan et al., 1965a]. There is no detectable instrumental drift among the detectors from these different satellites and the maximum difference in the absolute counting rate was less than 5%. This was easily corrected by using data from periods when two or more satellites overlapped in time. Figure 3 shows the cosmic ray omnidirectional intensity above 50 Mev measured by these GM counters from 1963 to 1965.

Using the differential energy spectrum measured in 1963, we have calculated for each ΔK the expected ratio I_{1965}/I_{1963} of the integral intensity above 50 Mev in 1965 to the corresponding intensity in 1963. This calculated ratio is shown as a function of ΔK in Figure 4. The value of this ratio obtained from the GM telescopes falls within the hatched horizontal band shown in the figure, and therefore we conclude that the value of ΔK should be roughly between 0.18 and 0.20. This is consistent with the value 0.20 used to characterize the change in the low energy differential spectrum between 1963 and 1965.

EXPERIMENTAL DATA DURING A PERIOD OF HIGH SOLAR ACTIVITY

During the period of high solar activity, the only suitable proton and He nucleus differential energy spectrum measurements were made by Webber and McDonald [1964], and Freier and Waddington [1965]. The energy spectra of protons and He nuclei (multiplied by 5) are shown in Figure 5. Below about 1 bev/nucleon the He nucleus spectrum is distinct from the proton spectrum. This situation is different from that at solar minimum where the spectra are essentially similar in a kinetic energy per nucleon representation.

From Parker's theory of the 11-year solar modulation, with the choice of $\sigma(\ell)$ and $N(\ell)$ given by equations 6 and 7, we have seen that the modulation is described by two different functions (equations 9 and 10). Although equation 9 predicts a modulation which is the same for protons and He nuclei, equation 10 depicts a different modulation for these two components. Written in terms of the velocity as it is done in (10), the difference between the proton and He nucleus modulation lies in the factor $(Z/A)^2$ in the exponent. If the value of (ℓ_0/R_0) is sufficiently low (such that the transition energy corresponding to the velocity β_0 is of the order of 100 Mev/nucleon), then we could expect that above this energy the He nuclei will be modulated less than the protons. Therefore the He nucleus intensity (after multiplication by 5) would be above the proton intensity and in qualitative agreement with the experimental observation. From the condition that $\beta_0 \leq 0.45$ for He nuclei (corresponding to a kinetic energy/nucleon of 100 Mev) we found that in 1959 $(\ell_0/R_0) \lesssim 1$. For $B = 5\gamma$ this implies $\ell_0 \lesssim 5 \times 10^{-3}$ AU.

Although this conclusion about the value of ℓ_0 can be reached by considering only the split between the proton and He nucleus spectra, a detailed fit of these spectra for various value of K and ℓ_0/R_0 is not possible. In order to investigate whether the origin of this difficulty lies in the assumption that the magnetic inhomogeneities have a scale size characterized by a single value ℓ_0 (equation 7), we have repeated the calculation using the following $\sigma(\ell, \beta)$ and $N(\ell)$:

$$\sigma(\ell, \beta) = \frac{\ell^2}{1 + (R/\ell)^2} \tag{15}$$

$$N(\ell) = 1/(2\pi)^{1/2}\, \ell_1 N \exp\left[-\frac{(\ell - \ell_0)^2}{2\ell_1^2}\right] \tag{16}$$

Equation 15 provides a continuous analytical expression for $\sigma(\ell, \beta)$, and in the limits of $R \ll \ell$ and $R \gg \ell$ it tends to the values given by equations 6a and 6b. Equation 16 represents a normalized gaussian distribution for $N(\ell)$ with a most probable value ℓ_0 and a variance ℓ_1^2. The normalization of $N(\ell)$ requires that

$$N_1 = \frac{1}{2}\left[1 + \mathrm{erf}\left(\frac{\ell_0}{\ell_1\sqrt{2}}\right)\right] \tag{17}$$

With this choice of $\sigma(\ell, \beta)$ and $N(\ell)$ we arrive at essentially the same results and conclusions reached from the simpler choice represented by (6) and (7). This is true for both periods of low and high solar activity.

PROTON TO HE NUCLEUS RATIO

We have used the forms of $\sigma(\ell, \beta)$ and $N(\ell)$ depicted by equations 15 and 16 to investigate the proton to He nucleus ratio as a function of energy throughout the solar cycle. With this choice, the modulation function can be written as

$$M(\beta) = \exp\left[-\frac{K'}{\beta}\, g(\beta,\, a,\, \xi,\, \eta)\right] \tag{18}$$

where

$$K' \equiv \frac{K}{(2\pi)^{1/2}\, N_1\, \eta} \tag{19}$$

$$g(\beta,\, a,\, \xi,\, \eta) \equiv \int_0^\infty x^4 \left[x^2 + (a\,\xi\,\gamma\,\beta)^2\right]^{-1} \exp\left[-\frac{(x-1)^2}{2\,\eta^2}\right] dx \tag{20}$$

$$a \equiv \frac{A}{Z}, \quad \xi \equiv \frac{R_0}{\ell_0}, \quad \eta \equiv \frac{\ell_1}{\ell_0} \quad \text{and} \quad \gamma \equiv (1-\beta^2)^{-1/2}$$

The proton to He nucleus ratio $R_{p\alpha}(r_e)$ at the earth's orbit for the same kinetic energy/nucleon can then be written as a function of the velocity of the particle:

$$R_{p\alpha}\,(r_e) = R_{p\alpha}\,(\infty)\, \exp\left[-\frac{K'}{\beta}\,(g_p - g_\alpha)\right] \tag{21}$$

where

$$g_p = g(\beta,\, 1,\, \xi,\, \eta), \quad g_\alpha = g(\beta,\, 2,\, \xi,\, \eta)$$

and $R_{p\alpha}(\infty)$ is the corresponding ratio outside the solar system.

The expressions g_p and g_α were integrated numerically from 10 Mev/nucleon to 10 bev/nucleon for different values of the parameter ξ. The parameter η was taken as 0.67.

Figure 6 presents the ratio $[R_{p\alpha}(r_e)/R_{p\alpha}(\infty)]$ as a function of the kinetic energy/nucleon for different values of K_L and ξ^{-1} $(\equiv \ell_0/R_0)$. K_L is defined by

$$K_L \equiv K' \ g\,(\beta = 0) \tag{22}$$

With this definition

$$M(\beta) \underset{\beta \to 0}{\rightarrow} \exp\,(-K_L/\beta) \tag{23}$$

for any ξ.

The measured values of $R_{p\alpha}(r_e)$ for 1961, 1963 and 1965 yield values for $(R_{p\alpha}(r_e)\,/\,R_{p\alpha}(\infty))$ all within the hatched area between curves A and C (Figure 6) providing we chose $R_{p\alpha}(\infty) \approx 6$. Figure 6 shows that, for the choice $R_{p\alpha}(r_e) = 6$, all the 1959 values for $R_{p\alpha}(r_e)/R_{p\alpha}(\infty)$ fall well outside the hatched area.

We conclude that the data on the proton to He nucleus ratio from 1959 through 1965, in the kinetic energy/nucleon interval of ~ 50 Mev to ~ 1 bev, are consistent with a constant proton to He nucleus ratio of 6 outside the solar system. From Figure 6 we also note that the 1961-1965 data are consistent with $(\ell_0/R_0) \geq 2$, and the 1959 with $(\ell_0/R_0) \leq 1$. Although the proton to He nucleus ratio during 1959 can be fitted with several different combinations of K_L and (ℓ_0/R_0) (see Figure 6), the actual proton spectrum generated with any of these combinations fails to agree with the experimental spectrum. In this connection it is of interest to note that energy losses in the expanding solar wind (neglected in the treatment presented in this paper) may be important [Parker, 1965]. For large values of K, characteristic of solar maximum, the actual intensity decrease could be much larger than that predicted by the simple theory. As the experimental data are too scarce, it has not been possible to draw any reliable conclusion regarding the role of energy losses in the modulation mechanism during the high solar activity period.

PROTON AND HE NUCLEUS RIGIDITY SPECTRA

Figures 7a, 7b, 7c and 7d show the proton and He nucleus (multiplied by 7.2) rigidity spectra during 1965, 1963, 1961 and 1959, respectively. During 1959 the proton and He nucleus spectra may be represented by the same curve, whereas during 1961, 1963 and 1965 there is a considerable split between these two components at low rigidities. This shows that during 1959 the modulation was essentially rigidity dependent down to about 600 Mv, indicating a small value of (ℓ_0/R_0) near solar maximum. On the other hand, during 1961, 1963 and 1965 any rigidity dependent modulation could occur only for rigidities $\geq$ 2 Bv, which indicates the large value of (ℓ_0/R_0) near solar minimum.

McCracken and Rao [1966], analyzing the average cosmic-ray solar diurnal anistropy obtained by means of neutron monitor data, arrive at the conclusion that the size and frequency of occurrence of the small scale irregularities in the interplanetary field did not change appreciably during the last solar cycle. We feel that this conclusion is not necessarily in contradiction with the views presented in this paper since the primary energies involved are different. In addition, the balloon and satellite data on which our conclusions are based refer to differential energy measurements, whereas the neutron monitor data reflect the integrated effect on particles with energy above ~1 bev.

Since (ℓ_0/R_0) changed by a factor of more than 2 from 1959 to the years near solar minimum (1961-1965), it is important to relate this cosmic ray observation to direct solar observations. In this connection we note that Babcock [1959] has observed that, during the middle of 1957, the polarity of the magnetic field near the south heliographic pole was reversed and that the field near the north pole was not seen to reverse until the end of 1958. There was a period of over a year when both the poles had the same polarity. Also, there was a six month period in 1957 when there was zero effective field. This unstable situation probably indicates a high overall turbulence giving rise to magnetic inhomogeneities with a wide range of scale sizes, including small values.

The evidence presented by Hewish [1958] on the basis of scattering of radio waves from the Crab Nebula when it is occulted by the solar corona also tends to show that the general scattering increases near the solar maximum. Though these inhomogeneities may be on a different scale, it is likely that the spectrum of turbulence tends to include a large number of smaller scale sizes.

CONCLUSIONS

1. During the period when the solar activity is low, in the interval 20 Mev/nucleon to 1 bev/nucleon, protons and He nuclei are modulated in a velocity dependent manner in reasonable accord with Parker's theory. The intensities during 1965 and 1961 are related to the intensity during 1963 by $I_{1965} = I_{1963} \times \exp(+0.2/\beta)$ and $I_{1961} = I_{1963} \times \exp(-0.4/\beta)$.

2. The parameter (ℓ_0/R_0) characterizing the magnetic turbulance during the solar minimum years 1961 - 1965 is equal to or greater than 2. During the period of high solar activity (1959) the existing data suggest that (ℓ_0/R_0) is less than 1.

3. The proton and He nucleus energy spectra near solar maximum derived from Parker's solar wind modulation theory, with a reasonable choice of parameters, cannot be made to fit the experimental observations. This suggests that energy losses in the expanding solar wind may be important near solar maximum.

4. By an examination of the data in the interval 20 to 1000 Mev/nucleon for the years 1961, 1963 and 1965, it is concluded that the proton to He nucleus intensity ratio $R_{p\alpha}(\infty)$ outside the solar system is approximately 6. This value is in close agreement with the universal abundance of these two elements. If this ratio increases at higher energies, as some measurements seem to indicate [Webber 1964], then there is a possibility that the proton and He nucleus spectra at the source are no

longer similar at higher energies. It is likely that a study of this ratio as a function of energy could give information on the mechanism of escape of these particles from the source regions.

ACKNOWLEDGMENTS

We thank Dr. F. B. McDonald for his encouragement and criticism and Dr. J. Lockwood for making available to us the Mt. Washington neutron monitor data.

APPENDIX

In deriving Formula 5 of the text we have assumed that the magnetic field B could be considered constant, equal to some effective value B_{eff}. Let us see now how this formula changes if we relax this restriction and let B be a function of the radial distance B(r). Then, for any distribution of the scale size of the inhomogeneities $N(\ell)$ we have for the modulation function

$$M(\beta) = \exp\left\{-\frac{1}{\beta}\left[\int_{r_e}^{\infty} \frac{3V(r)\,n(r)}{c} \cdot \left(\int_0^{\infty} \sigma(\ell, \beta, r)\,N(\ell)\,d\ell\right) dr\right]\right\} \tag{A1}$$

where the cross section $\sigma(\ell, \beta, r)$ now depends also on the radial distance r through its dependence on the magnetic field B(r).

In order to see in more detail what influence B(r) and $N(\ell)$ will have on $M(\beta)$ let us assume that

$$\sigma(\ell, \beta, r) = \ell^2 \text{ when } \beta \to 0 \tag{A2}$$

and

$$\sigma(\ell, \beta, r) = (\ell^4/R^2) \text{ when } \beta \to 1 \tag{A3}$$

in agreement with (6a) and (6b). Then we obtain

$$\int_0^{\infty} \sigma(\ell, \beta, r)\,N(\ell)\,d\ell = \int_0^{\infty} \ell^2\,N(\ell)\,d\ell \equiv \langle \ell^2 \rangle \text{ when } \beta \to 0 \tag{A4}$$

$$\int_0^{\infty} \sigma(\ell,\ \beta,\ r)\, N(\ell)\, d\ell = \frac{1}{R^2}\int_0^{\infty} \ell^4\, N(\ell)\, d\ell \equiv \frac{1}{R^2} < \ell^4 > \text{ when } \beta \to 1 \qquad \text{(A5)}$$

and thus

$$\underset{\beta \to 0}{M(\beta)} = \exp\left[-\frac{1}{\beta} < \ell^2 > \int_{r_e}^{\infty} \frac{3\,V(r)\, n(r)}{c}\, dr\right] \qquad \text{(A6)}$$

$$\underset{\beta \to 0}{M(\beta)} = \exp\left\{-\frac{(1-\beta^2)}{\beta^3} \cdot \left(\frac{Z}{A}\right)^2 \cdot \frac{< \ell^4 >}{R_0^2} \cdot \int_{r_e}^{\infty} \frac{3\,V(r)}{c} \cdot \left[\frac{B(r)}{B_e}\right]^2 n(r)\, dr\right\} \qquad \text{(A7)}$$

where now $R_0 = mc^2/eB_e$ and $B_e = B(r_e)$.

From this, we can see the effect that $N(\ell)$ and $B(r)$ have on the low- and high-energy approximation formulas for $M(\beta)$ (equations A6 and A7). The effect of choosing different forms for the distribution function $N(\ell)$ is felt through the different values that $< \ell^2 >$ and $< \ell^4 >$ will have in the low- and high-energy approximations. The choice of the function $B(r)$ will not affect (A6) but introduce a variation in (A7) through the term

$$\int_{r_e}^{\infty} \frac{3\,V(r)}{c} \cdot \left[\frac{B(r)}{B_e}\right]^2 n(r)\, dr$$

where different values for $B(r)$ will result in different values for this integral.

If we now specify

$$N(\ell) = \frac{1}{(2\pi)^{1/2}\,\ell_1\,N_1}\,\exp\left[-\frac{(\ell-\ell_0)^2}{2\ell_1^2}\right]$$

then

$$\underset{\beta\to 0}{M(\beta)} = \exp\left[-\frac{1}{\beta}\cdot\ell_0^2\,(1+\eta^2+b\eta)\int_{r_e}^{\infty}\frac{3V(r)\,n(r)}{c}\,dr\right]$$

$$= \exp\left[-\frac{K(1+\eta^2+b\eta)}{\beta}\right] \qquad \text{(A8)}$$

and

$$\underset{\beta\to 1}{M(\beta)} = \exp\left\{-\frac{(1-\beta^2)}{\beta^3}\cdot\left(\frac{Z}{A}\right)^2\cdot\left(\frac{\ell_0}{R_0}\right)^2\ell_0^2\left[1+6\eta^2+3\eta^4+b(\eta+5\eta^3)\right]\right.$$

$$\left.\cdot\int_{r_e}^{\infty}\frac{3V(r)}{c}\left[\frac{B(r)}{B_e}\right]^2 n(r)\,dr\right\}$$

$$= \exp\left\{-\frac{(1-\beta^2)}{\beta^3}\cdot\left(\frac{Z}{A}\right)^2\left(\frac{\ell_0}{R_0}\right)^2 K_1\left[1+6\eta^2+3\eta^4+b(\eta+5\eta^3)\right]\right\} \qquad \text{(A9)}$$

where

$$b = \frac{1}{(2\pi)^{1/2}\,N_1\,\exp(1/2\,\eta^2)}\,, \qquad \eta = \frac{\ell_1}{\ell_0}$$

$$K = \ell_0^2\int_{r_e}^{\infty}\frac{3V(r)\,n(r)}{c}\,dr\,, \text{ and } K_1 = \ell_0^2\int_{r_e}^{\infty}\frac{3V(r)}{c}\cdot\left[\frac{B(r)}{B_e}\right]^2 n(r)\,dr$$

If in addition $B(r)$ = constant = B_e, then K_1 = K and equations A8 and A9 would agree with the low- and high-energy limits of (19) given in the text.

On the other hand if

$$N(\ell) = \delta(\ell - \ell_0)$$

then

$$\underset{\beta \to 0}{M(\beta)} = \exp\left(-\frac{K}{\beta}\right) \tag{A10}$$

$$\underset{\beta \to 1}{M(\beta)} = \exp\left[-\frac{(1-\beta^2)}{\beta^3}\left(\frac{Z}{A}\right)^2\left(\frac{\ell_0}{R_0}\right)^2 K_1\right] \tag{A11}$$

And again if $B(r)$ = constant = B_e, then $K = K_1$ and equations A10 and A11 agree with (9) and (10) of this paper.

REFERENCES

Babcock, H. D., The sun's polar magnetic field, Ap.J.,130, 364-365, 1959.

Balasubrahmanyan, V. K. and F. B. McDonald, Solar modulation effects on the primary cosmic radiation near solar minimum, J. Geophys. Res., 69, 3289-3292, 1964.

Balasubrahmanyan, V. K., G. H. Ludwig, F. B. McDonald, and R. A. R. Palmeira, Results from the IMP-I GM counter telescope experiment, J. Geophys. Res., 70, 2005-2019, 1965a.

Balasubrahmanyan, V. K., E. Boldt, and R. A. R. Palmeira, Low-energy spectrum of cosmic rays as an indicator of primary source characteristics and interstellar propagation, Phys. Rev., 140, B1157-B1161, 1965b.

Balasubrahmanyan, V. K., D. E. Hagge, G. H. Ludwig, and F. B. McDonald, Galactic cosmic rays at solar minimum, 1965, Proc. London, Cosmic-Ray Conference (In Press), 1965c.

Bonetti, A., H. S. Bridge, A. J. Lazarus, B. Rossi and F. Scherb, Explorer 10 plasma measurements, J. Geophys. Res., 68, 4017-4063, 1963.

Bryant, D. A., T. L. Cline, U. D. Desai, and F. B. McDonald, Explorer XII observations of solar cosmic rays and energetic storm particles following the solar flare of 28 September 1961, J. Geophys. Res., 17, 4983-5000, 1962.

Fan, C. Y., G. Gloeckler, and J. A. Simpson, Cosmic radiation helium spectrum below 90 Mev per nucleon measured on IMP-I satellite, J. Geophys. Res., 70, 3515-3527, 1965a.

Fan, C. Y., G. Gloeckler, and J. A. Simpson, Protons and helium nuclei within interplanetary magnetic regions which co-rotate with the sun, Proc. London Cosmic-Ray Conference, (In press) 1965b.

Fichtel, C. E., N. Durgaprasad, and D. E. Guss, 1961-1964 balloon observations of cosmic rays, Goddard Space Flight Center Document X-611-65-379, 1965.

Forbush, S. E., Worldwide cosmic ray variations, J. Geophys. Res., 59, 525-542, 1954.

Freier, P. S. and C. J. Waddington, The helium nuclei of the primary cosmic radiation as studied over a solar cycle of activity interpreted in terms of electric field modulation, Space Sci. Rev., IV, 313-372, 1965.

Gleockler, G., Solar modulation of the low-energy galactic helium spectrum as observed on the IMP-I satellite, J. Geophys. Res., 70, 5333-5343, 1965.

Hewish, A., The scattering of radio waves in the solar corona, Mot. Not. Roy. Astron. Soc., 118, 534-546, 1958.

McCracken, K. G. and U. R. Rao, The temporal independence of the occurrence of small scale irregularities in the interplanetary magnetic field, (In preparation) 1966.

McDonald, F. B. and G. H. Ludwig, Measurements of the low energy primary cosmic ray protons on IMP-I satellite, Phys. Rev. Letters, Dec. 28, 1964.

Meyer, P. and R. Vogt, Primary cosmic ray and solar protons. II, Phys. Rev. 129, 2275-2279, 1963.

Nagashima, K. S., P. Duggal, and M. A. Pomerantz, Long term modulation of primary cosmic ray intensity, Planet. Space Sci., 14, 177-206, 1965.

Ness, N. F., C. L. Scearce, and J. B. Seek, Initial results of the IMP-I magnetic field experiment, J. Geophys. Res., 69, 3531-3569, 1964.

Ness, N. F. and J. W. Wilcox, Extension of the photospheric magnetic field into interplanetary space, Ap. J., 143, 23-31, 1966.

Parker, E. N., Interplanetary Dynamic Processes, John Wiley & Sons, New York, 1963.

Parker, E. N., The passage of energetic charged particles through interplanetary space, Planet. Space Sci., 13, 9-49, 1965.

Quenby, J. J., The time variation of the cosmic ray intensity (In press) 1964.

Webber, W. R., The spectrum and charge composition of the primary cosmic radiation, University of Minnesota Technical Report CR-76, 1964.

Webber, W. R. and F. B. McDonald, Cerenkov scintillation counter measurements of the intensity and modulation of low rigidity cosmic rays and features of the geomagnetic cutoff rigidity, J. Geophys. Res., 69, 3097-3114, 1964.

FIGURE CAPTIONS

Fig. 1. Sunspot number and Mt. Washington neutron monitor rate during solar cycle 19. The arrows indicate the times of balloon flights from which the data used in this paper were obtained. The hatched region shows the time of satellite coverage.

Fig. 2. Proton and He nucleus (x5) energy spectra measured by balloons and satellites during 1961, 1963, and 1965. The 1961 data are from Fichtel et al. [1965], Bryant et al. [1962], and Meyer and Vogt [1963]. The 1963 data are from the following sources: McDonald and Ludwig [1964], Fan et al. [1965a], and Balasubrahmanyan and McDonald [1964]. The 1965 data are from Balasubrahmanyan et al. [1965c]. The lowest energy He nucleus data point exhibited for 1965 might have a contribution associated with long-lived solar streams [Fan et al, 1965b].

Fig. 3. The total integral intensity of cosmic rays above 50 Mev as measured by GM counters on IMP-I, II, III and OGO-I satellites.

Fig. 4. The ratio I_{1965}/I_{1963} of the 1965 to the 1963 total cosmic ray integral intensity above 50 Mev as a function of the increment ΔK in the parameter K of the solar wind modulation theory. The experimentally observed ratio I_{1965}/I_{1963} falls within the hatched area.

Fig. 5. The proton and He nucleus (x5) energy spectrum during 1959. The data are from Webber and McDonald [1964], and Freier and Waddington [1965]. The smooth curve that fits the 1963 data is shown for comparison.

Fig. 6. The relative proton to He nucleus ratio inside the solar system as a function of the kinetic energy per nucleon according to the solar wind modulation theory, and with the choice of the distribution of the scale size of the magnetic inhomogeneities given in the text. See also the text for the definition of the parameters K_L and ℓ_0/R_0.

Fig. 7a. The proton and He nucleus (x7.2) rigidity spectra during 1965. The data are the same as in Figure 2.

Fig. 7b. The proton and He nucleus (x7.2) rigidity spectra during 1963. The data are the same as in Figure 2.

Fig. 7c. The proton and He nucleus (x7.2) rigidity spectrum during 1961. The data are the same as in Figure 2.

Fig. 7d. The proton and He nucleus (x7.2) rigidity spectrum during 1959. The data are the same as in Figure 5.

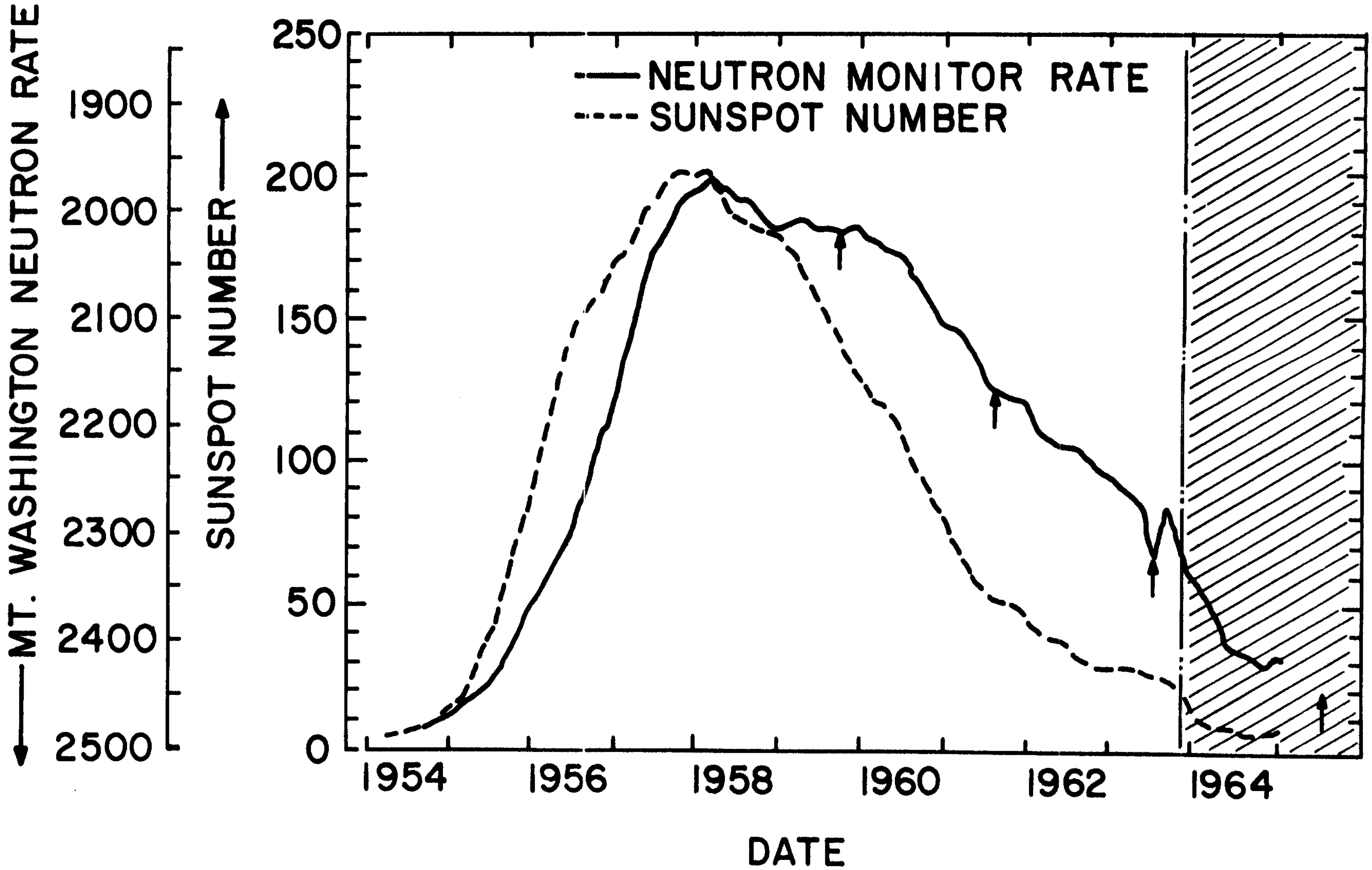

MT. WASHINGTON NEUTRON RATE
1900
2000
2100
2200
2300
2400
2500
SUNSPOT NUMBER
250
200
150
100
50
0
NEUTRON MONITOR RATE
SUNSPOT NUMBER
1954
1956
1958
1960
1962
1964
DATE

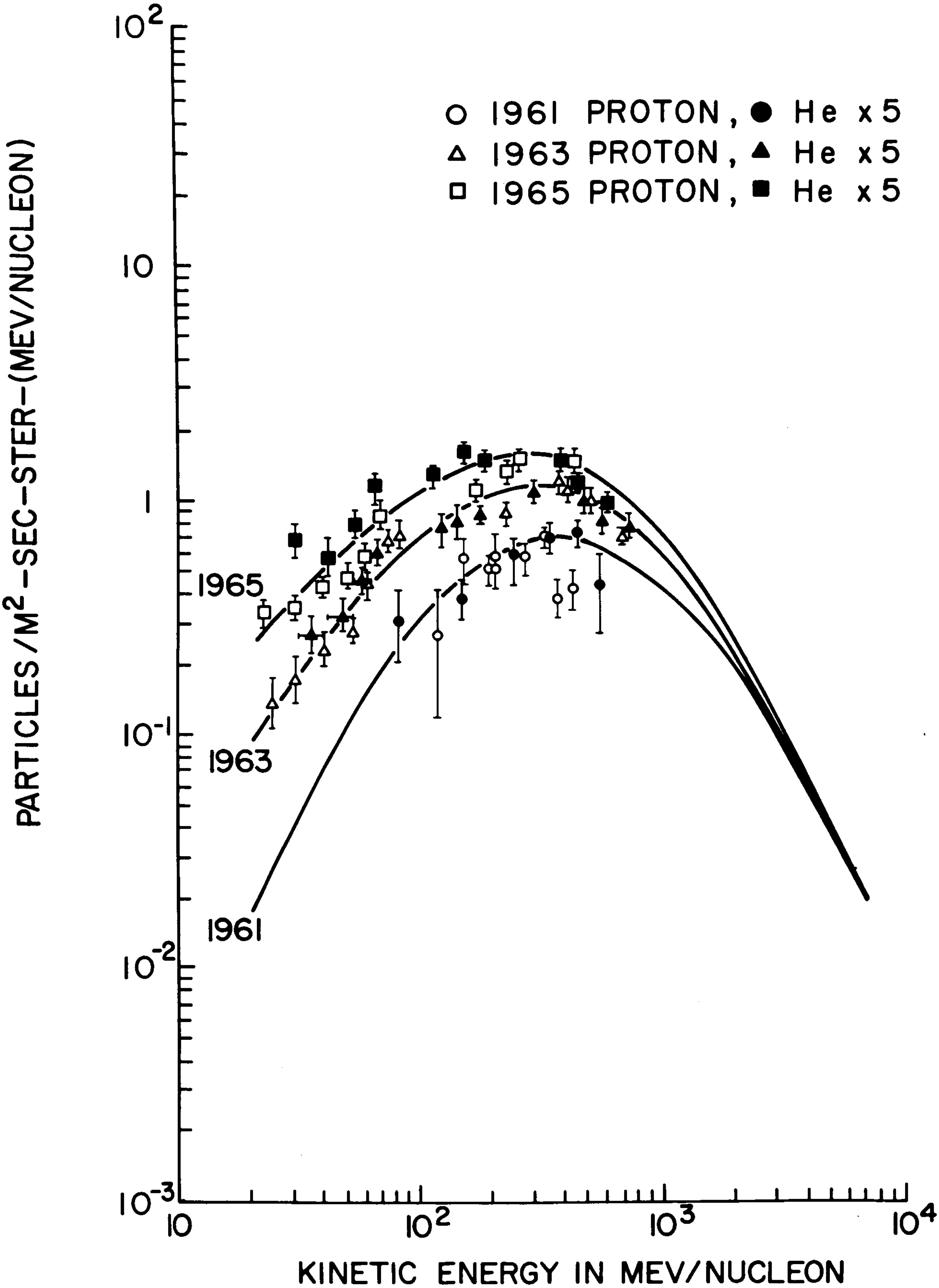
○ 1961 PROTON, ● He x5
△ 1963 PROTON, ▲ He x5
□ 1965 PROTON, ■ He x5
1965
1963
1961
PARTICLES/M2-SEC-STER-(MEV/NUCLEON)
KINETIC ENERGY IN MEV/NUCLEON
10^2
10
1
10^-1
10^-2
10^-3
10
10^2
10^3
10^4

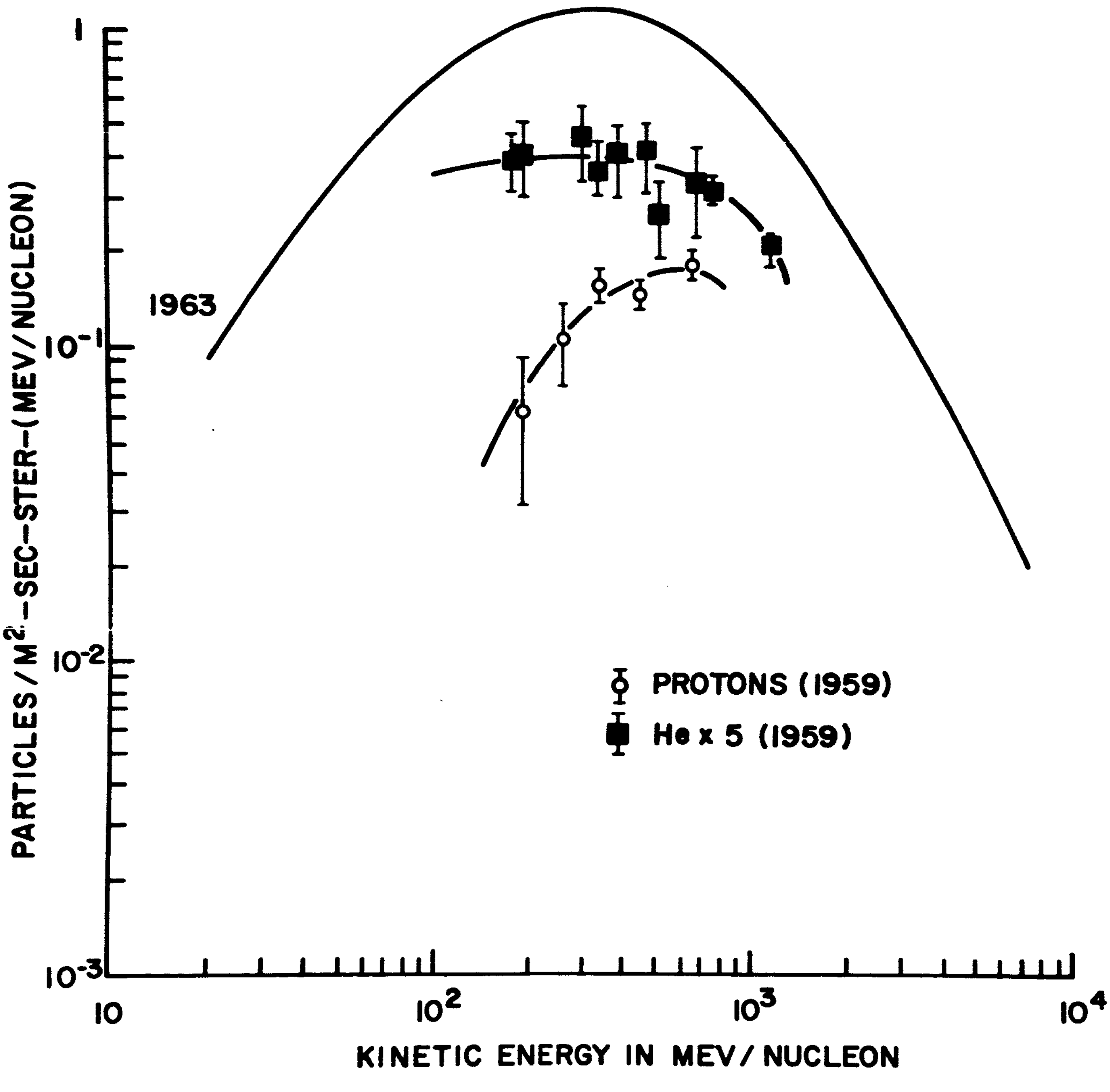

1963
PROTONS (1959)
He x 5 (1959)
PARTICLES/M²-SEC-STER-(MEV/NUCLEON)
KINETIC ENERGY IN MEV/NUCLEON
1
10⁻¹
10⁻²
10⁻³
10
10²
10³
10⁴

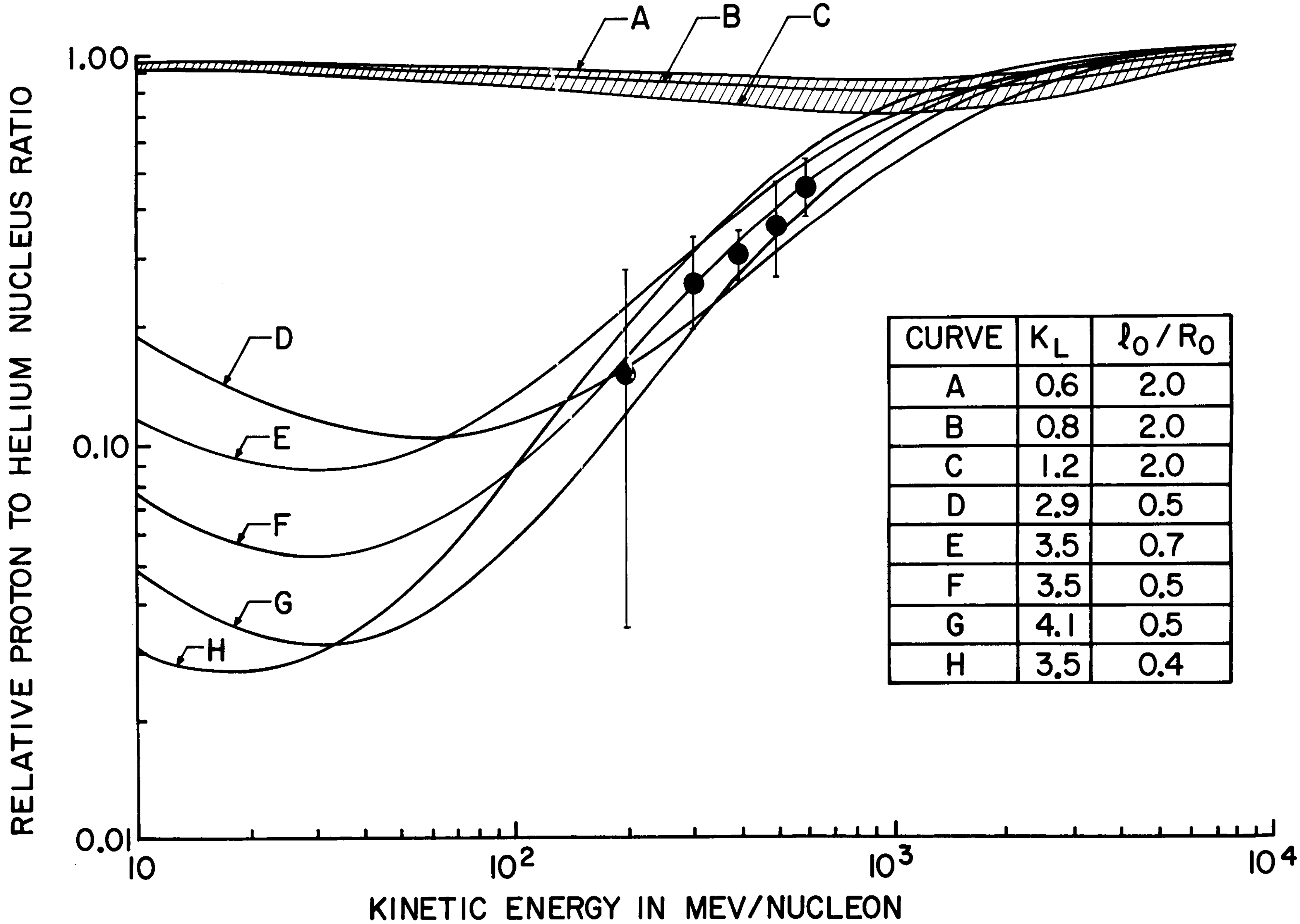

A
B
C
D
E
F
G
H
1.00
0.10
0.01
10
10^2
10^3
10^4
RELATIVE PROTON TO HELIUM NUCLEUS RATIO
KINETIC ENERGY IN MEV/NUCLEON

CURVE	K_L	l_0/R_0
A	0.6	2.0
B	0.8	2.0
C	1.2	2.0
D	2.9	0.5
E	3.5	0.7
F	3.5	0.5
G	4.1	0.5
H	3.5	0.4

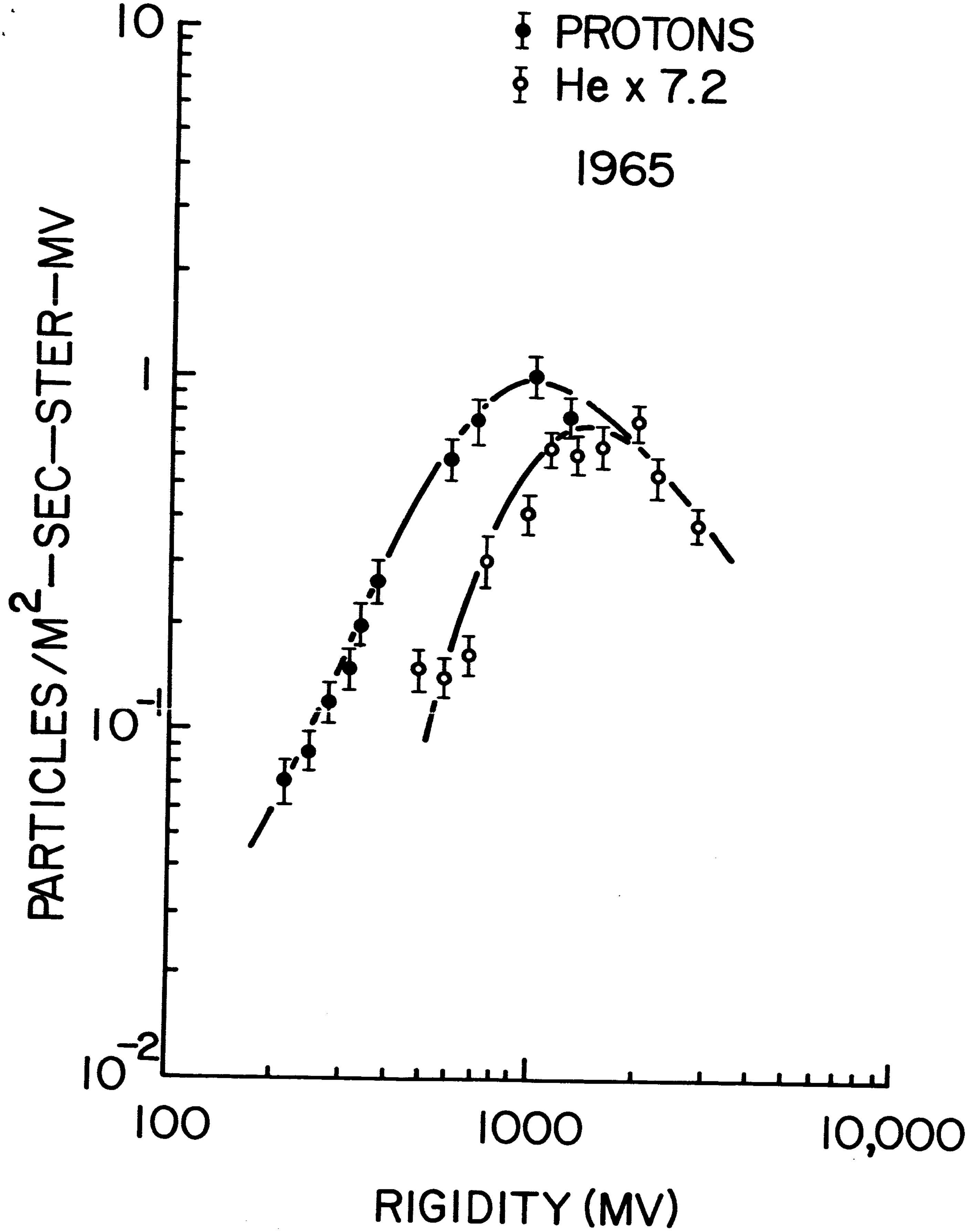
PROTONS
He x 7.2
1965
PARTICLES/M2—SEC—STER—MV
10
1
10-1
10-2
100
1000
10,000
RIGIDITY (MV)

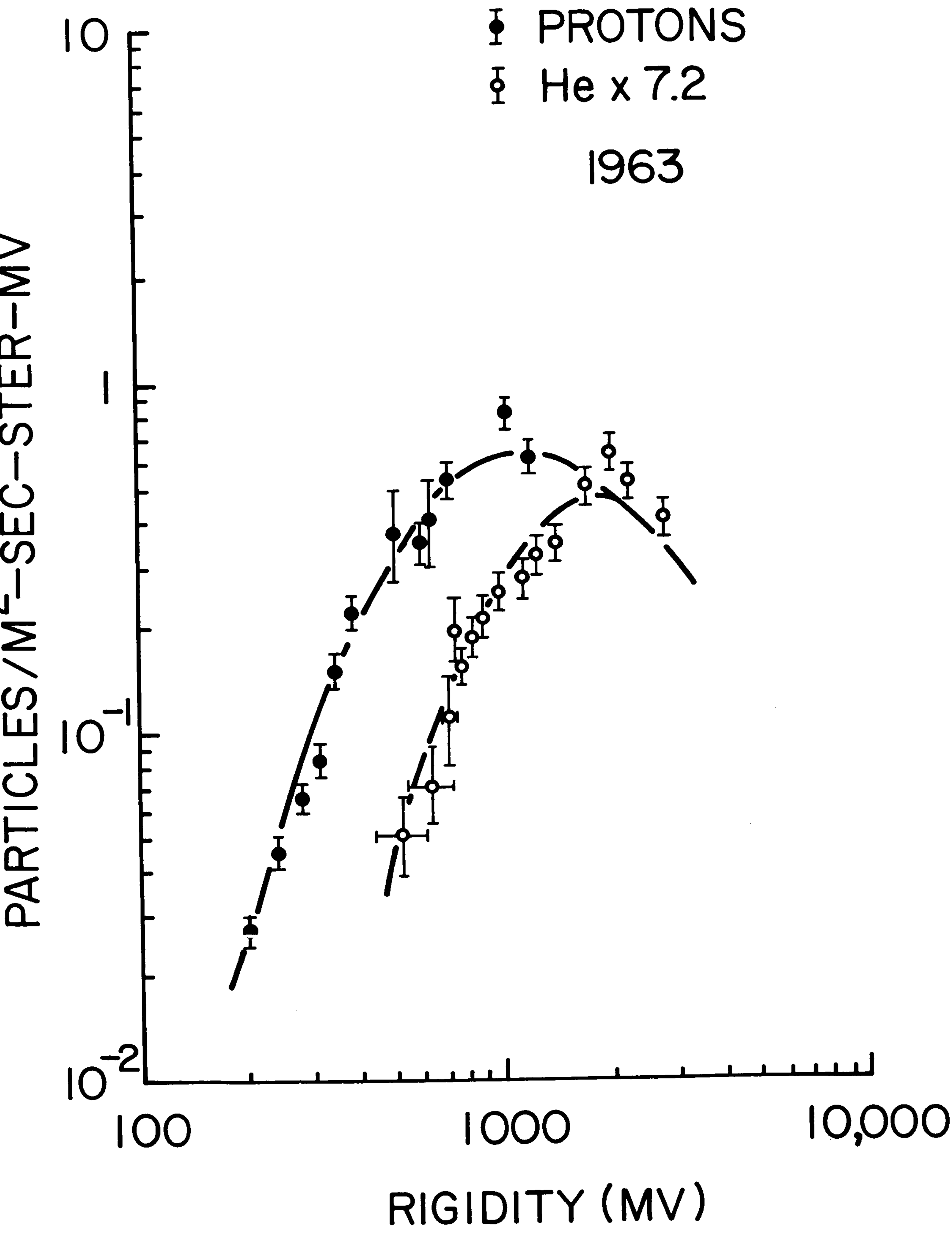
PROTONS
He x 7.2
1963
PARTICLES/M2–SEC–STER–MV
10
1
10^{-1}
10^{-2}
100
1000
10,000
RIGIDITY (MV)

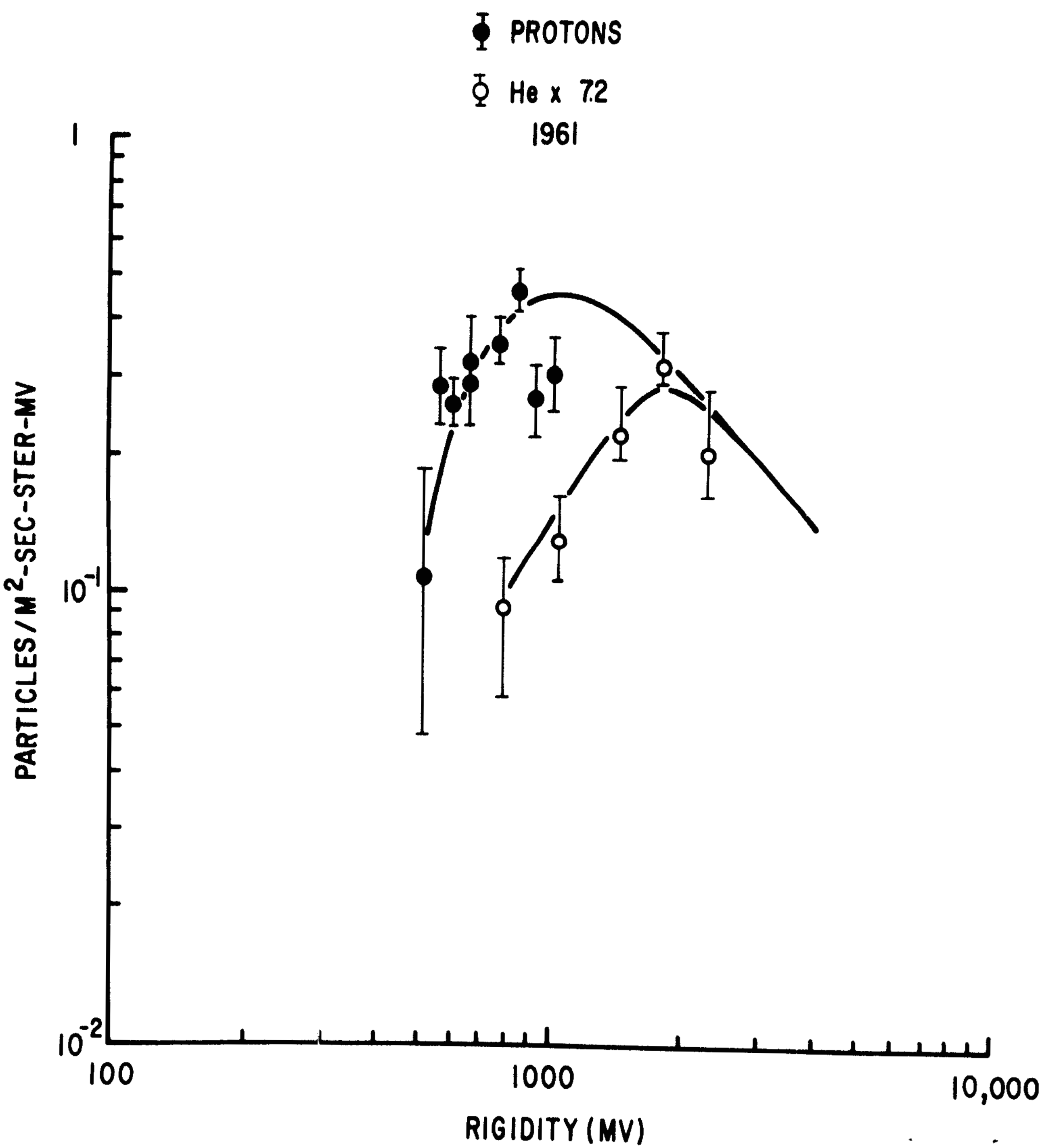
PROTONS
He x 7.2
1961
1
10^{-1}
10^{-2}
PARTICLES/M^2-SEC-STER-MV
100
1000
10,000
RIGIDITY (MV)

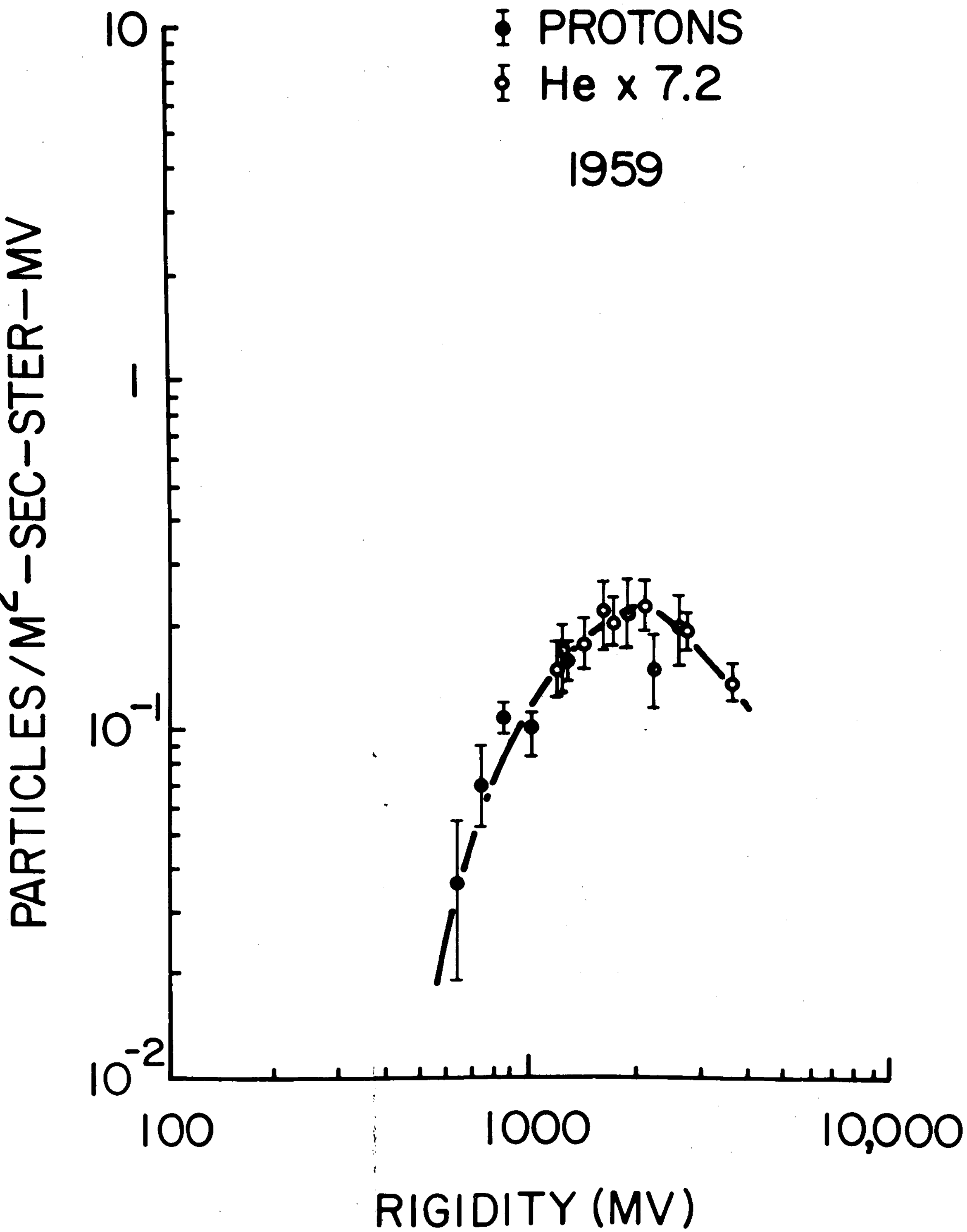
PROTONS
He x 7.2
1959
PARTICLES/M^2-SEC-STER-MV
10
1
10^{-1}
10^{-2}
100
1000
10,000
RIGIDITY (MV)